JOURNAL OF CATALYSIS 114, 230–245 (1988)

CH_3NH_2 Decomposition and Oxidation on Polycrystalline Platinum: Steady-State Kinetics and Oscillations[1]

S. Y. HWANG AND L. D. SCHMIDT

Department of Chemical Engineering and Material Science, University of Minnesota, Minneapolis, Minnesota 55455

Received January 4, 1988; revised May 26, 1988

Steady-state rates of decomposition and oxidation of methylamine on polycrystalline platinum between 600 and 1500 K have been studied in a mixed reactor with methylamine and oxygen partial pressures from 0.2 to 6 Torr. HCN and H_2 are the dominant products (>98%) in excess methylamine. In excess oxygen, CO, N_2O, NO, and H_2O increase but HCN remains the major product up to a twofold excess of oxygen. Less than 2% of CH_4, NH_3, CO_2, or C_2N_2 is produced under any conditions. Reaction rates rise rapidly up to ~950 K, and most reactions appear to become flux limited by ~1100 K. The reaction probability of methylamine at high temperature varies from 0.025 in a 4/1 methylamine excess to 0.010 in 2/1 oxygen excess. The reaction probabilities of oxygen are ~0.003 and are independent of methylamine pressure. These results suggest that $CH_3NH_2 \rightarrow$ HCN is the dominant reaction channel even in excess oxygen and that oxygen mostly reacts with atomic hydrogen but does not significantly affect the C–N bond in CH_3NH_2. Oscillations of wire temperature and reactor pressure occur at excess methylamine, while multiple steady states are observed in excess oxygen. These are caused by heat effects of the endothermic decomposition reaction and the exothermic oxidation reaction.

1. INTRODUCTION

The reactions of aliphatic amines over metal catalysts have been studied previously by several groups (*1–14*) using catalysts in the form of metal films, metal powders, supported catalysts, and single crystals. It has been shown that when mixtures of methylamine and hydrogen were contacted with evaporated Pt, Pd, Ni, Fe, W, Co, V, and Cu films at total pressure of 30–35 Torr between 410 and 640 K, the most common reaction products were ammonia, methane, and dimethylamine (*3, 6*). Small amount of products such as trimethylamine, acetonitrile, ethylenimine, and C_2–C_4 hydrocarbons were observed.

Meitzner *et al.* (*8*) studied the methylamine reactions in the presence of hydrogen between 360 and 770 K over a number of metals supported on silica. They observed no significant production of HCN and reported that for supported Pt between 450 and 540 K, dimethylamine formation was up to two times greater than that of methane. Methylamine adsorption and reaction on single-crystal surfaces have also been studied by TPD and AES on Pt(111) (*9, 10*) and Ni(111) (*11*); by TPD on W(100) (*12*); by LEED, AES, and TPD on Mo(100) (*13*); and by EELS on Ni(100), Ni(111), Cr(100), and Cr(111) (*14*).

The oxidation of ammonia over metal catalysts has also been studied extensively (*15–22*), with major products found to be nitric oxide, nitrogen, and water. Flytzani-Stephanopoulos *et al.* (*15*) reported an experimental study of temperature oscillations of platinum wires and foils in ammonia oxidation at atmospheric pressure. Oscillations with periods from less than 1 s to several minutes were obtained for gas composition between 20 and 40% NH_3 in air.

In this study, we examine the decomposi-

[1] This work partially supported by the National Science Foundation under Grant DMR82126729.

0021-9517/88 $3.00

tion and oxidation of methylamine over polycrystalline platinum wires. Several reactions are possible in a mixture of methylamine and oxygen:

dehydrogenation

$$CH_3NH_2 \rightarrow HCN + 2\,H_2, \quad \Delta H = +36{,}700 \quad (1)$$

$$CH_3NH_2 \rightarrow \tfrac{1}{2}C_2N_2 + \tfrac{5}{2}H_2, \quad \Delta H = +42{,}420 \quad (2)$$

hydrogenolysis

$$CH_3NH_2 + H_2 \rightarrow CH_4 + NH_3, \quad \Delta H = -23{,}310 \quad (3)$$

cracking

$$CH_3NH_2 \rightarrow \tfrac{1}{2}N_2 + CH_4 + \tfrac{1}{2}H_2, \quad \Delta H = -12{,}390 \quad (4)$$

oxidative dehydrogenation

$$CH_3NH_2 + O_2 \rightarrow HCN + 2\,H_2O, \quad \Delta H = -78{,}900 \quad (5)$$

$$CH_3NH_2 + \tfrac{5}{4}O_2 \rightarrow \tfrac{1}{2}C_2N_2 + \tfrac{5}{2}H_2O, \quad \Delta H = -102{,}100 \quad (6)$$

oxidative cracking

$$CH_3NH_2 + \tfrac{7}{4}O_2 \rightarrow \tfrac{1}{2}N_2 + CO + \tfrac{5}{2}H_2O, \quad \Delta H = -165{,}425 \quad (7)$$

All Heats of reaction are in calories per mole CH_3NH_2 calculated at 298 K. In the presence of oxygen and water, some products can be further reacted in reactions listed in Table 1. Although the system has at least 25 possible reactions, many of them have been studied previously (*20–30*) and rate expressions have been developed over polycrystalline platinum wires or foils as indicated and observed order measured at 1 Torr of each reactant. We shall use these rate expressions to consider the possible contribution of these reactions to the methylamine–oxygen system.

2. EXPERIMENTAL

Experiments were performed in a combined ultrahigh-vacuum–high-pressure reactor system described previously (*20*). A sample could be transferred under ultrahigh vacuum ($<1 \times 10^{-8}$ Torr) from the UHV analysis chamber to the reactor using two

TABLE 1

Possible Reactions in $CH_3NH_2 + O_2$

Possible reaction	$\Delta H°_{298}$ (cal/mol)	Observed order[a]	Reference
(8) $NH_3 + \frac{5}{4}O_2 \rightarrow NO + \frac{3}{2}H_2O$	−54,180	$P_{NH_3}P_{O_2}^{1/2}$	(*21, 22*)
(9) $NH_3 + \frac{3}{4}O_2 \rightarrow \frac{1}{2}N_2 + \frac{3}{2}H_2O$	−75,780	$P_{NH_3}P_{O_2}^{-1}$	(*21, 22*)
(10) $CH_4 + \frac{3}{2}O_2 \rightarrow CO + 2H_2O$	−124,130	$P_{CH_4}P_{O_2}^{1/2}$	(*20*)
(11) $CH_4 + 2O_2 \rightarrow CO_2 + 2H_2O$	−191,760	$P_{CH_4}P_{O_2}$	(*20*)
(12) $HCN + \frac{3}{4}O_2 \rightarrow CO + \frac{1}{2}N_2 + \frac{1}{2}H_2O$	−86,525		
(13) $H_2 + \frac{1}{2}O_2 \rightarrow H_2O$	−57,800	$P_{O_2}P_{H_2}$	(*30*)
(14) $CO + \frac{1}{2}O_2 \rightarrow CO_2$	−67,650	$P_{CO}P_{O_2}^{-1}$	(*28, 30*)
(15) $NO + H_2 \rightarrow \frac{1}{2}N_2 + H_2O$	−79,400	P_{NO}	(*27*)
(16) $HCN + H_2O \rightarrow NH_3 + CO$	−10,740		
(17) $CO + H_2O \rightarrow CO_2 + H_2$	−9,830	$P_{CO}P_{H_2O}^{1/2}$	(*30*)
(18) $NH_3 \rightarrow \frac{1}{2}N_2 + \frac{3}{2}H_2$	10,920	P_{NH_3}	(*25, 27*)
(19) $HCN \rightarrow \frac{1}{2}C_2N_2 + \frac{1}{2}H_2$	5,720		
(20) $NO \rightarrow \frac{1}{2}N_2 + \frac{1}{2}O_2$	−21,600	$P_{NO}P_{O_2}^{-1}$	(*26, 27*)
(21) $NO + \frac{2}{3}NH_3 \rightarrow \frac{5}{6}N_2 + H_2O$	−72,120	$P_{NO}P_{NH_3}^{1/2}$	(*29*)
(22) $CH_4 + NH_3 \rightarrow HCN + 3H_2$	60,010	$P_{CH_4}P_{NH_3}^{1/2}$	(*20, 23*)
(23) $CH_4 + 3NO \rightarrow \frac{3}{2}N_2 + CO + H_2O$	−131,150	$P_{NO}P_{CH_4}^{1/2}$	(*20*)
(24) $CH_4 + NO \rightarrow HCN + \frac{1}{2}H_2 + H_2O$	−30,310	$P_{NO}P_{CH_4}$	(*20*)
(25) $NO + CO \rightarrow \frac{1}{2}N_2 + CO_2$	−89,250	P_{NO}	(*24, 28*)

[a] Reaction orders measured at ~1 Torr of each reactant.

magnetically coupled rods. The reaction chamber was constructed using two stainless-steel six-way crosses attached through a gate value to the ion and sublimation pumped UHV system containing a mass and an Auger spectrometer for residual gas and surface analysis. The platinum wire was spot-welded to a stainless-steel plug which had four insulated pins for resistive heating and temperature measurements using a Pt–Rh thermocouple spot-welded to the center of the wire. The resistance of the wire was measured in some experiments to calculate the average temperature of the wire. As discussed later, the average and center temperatures can be quite different and are influenced by reaction.

The plug was attached to a feedthrough either in the UHV system for surface analysis or in the reactor for kinetic studies. The methylamine and oxygen pressures were adjusted by metering valves and were pumped with a trapped mechanical vacuum pump. The residence time in the reactor could be varied from 0.3 to 10 s with a butterfly valve between the reactor and the pump. Total pressures were recorded with a capacitance manometer in the reactor.

The composition of the gas in the reactor was determined by leaking gases into the UHV system at $\sim 5 \times 10^{-8}$ Torr. The mass spectrometer sensitivities of all the reactants and products were calibrated against an ionization gauge in the UHV chamber. The absolute mass spectrometer sensitivities for H_2, N_2, O_2, CO, H_2O, CO_2, and NO were then obtained by calibrating against known ionization gauge sensitivities for these gases. The ionization gauge sensitivities for HCN, NH_3, C_2N_2, and CH_3NH_2 were assumed to be the same as that of nitrogen. Cracking patterns of all reactants and products were also calibrated under the experimental condition without reaction to identify products and calculate reaction rates.

The platinum wire (0.25 mm in diameter, ~5 cm long, 99.95%, Alfa) was cleaned by heating in 5 Torr of oxygen at 1400 K and in UHV at 1600 K until AES showed no evidence of impurities. The methylamine (>98.5%) contained <0.8% of dimethylamine and trimethylamine, <0.15% water, and <0.01% ammonia. Oxygen (99.995%) was used without further purification.

3. RESULTS

3.1. Rates versus Wire Temperature

Figures 1a through 1d show the rates of consumption of CH_3NH_2 and O_2 and the rates of formation of H_2, HCN, NH_3, H_2O, and 28 amu (CO and N_2) as functions of the current applied to the wire at 2 Torr of methylamine with 0.25, 1.0, 2.0, and 4.0 Torr of oxygen. Figures 1a and 1b show that at low oxygen partial pressure all rates increase smoothly with increasing current up to a flux-limited plateau and then level off except for 28 amu and NH_3 which continue to rise. However, at higher oxygen partial pressure, Figs. 1c and 1d show that no reaction occurs until the wire is heated to some critical temperatures where the reactions are ignited to a state very close to the high-temperature flux-limited plateau which the system eventually attains. Similar sets of data were obtained with 1 Torr of methylamine. Qualitatively identical behavior was observed for methylamine pressures from 0.5 to 6 Torr in that HCN was the major product and the rate rose discontinuously if $P_{O_2}/P_{CH_3NH_2}$ was greater than unity.

At $P_{O_2}/P_{CH_3NH_2}$ ratios less than unity, the rate of formation of HCN is nearly identical to the rate of consumption of methylamine, indicating that Eq. (1) is the major reaction. The rate of H_2 production follows this trend, although the H_2 sensitivity was lower by a factor of 1.6 and was calibrated from Eq. (1) at low oxygen partial pressure. In excess oxygen, Fig. 1d shows that about 70% of the amine reacts to form HCN and the rest forms mainly CO and N_2. Very little (<1%) C_2N_2 and CO_2 were formed under any condition.

Figure 2a shows the temperature of the

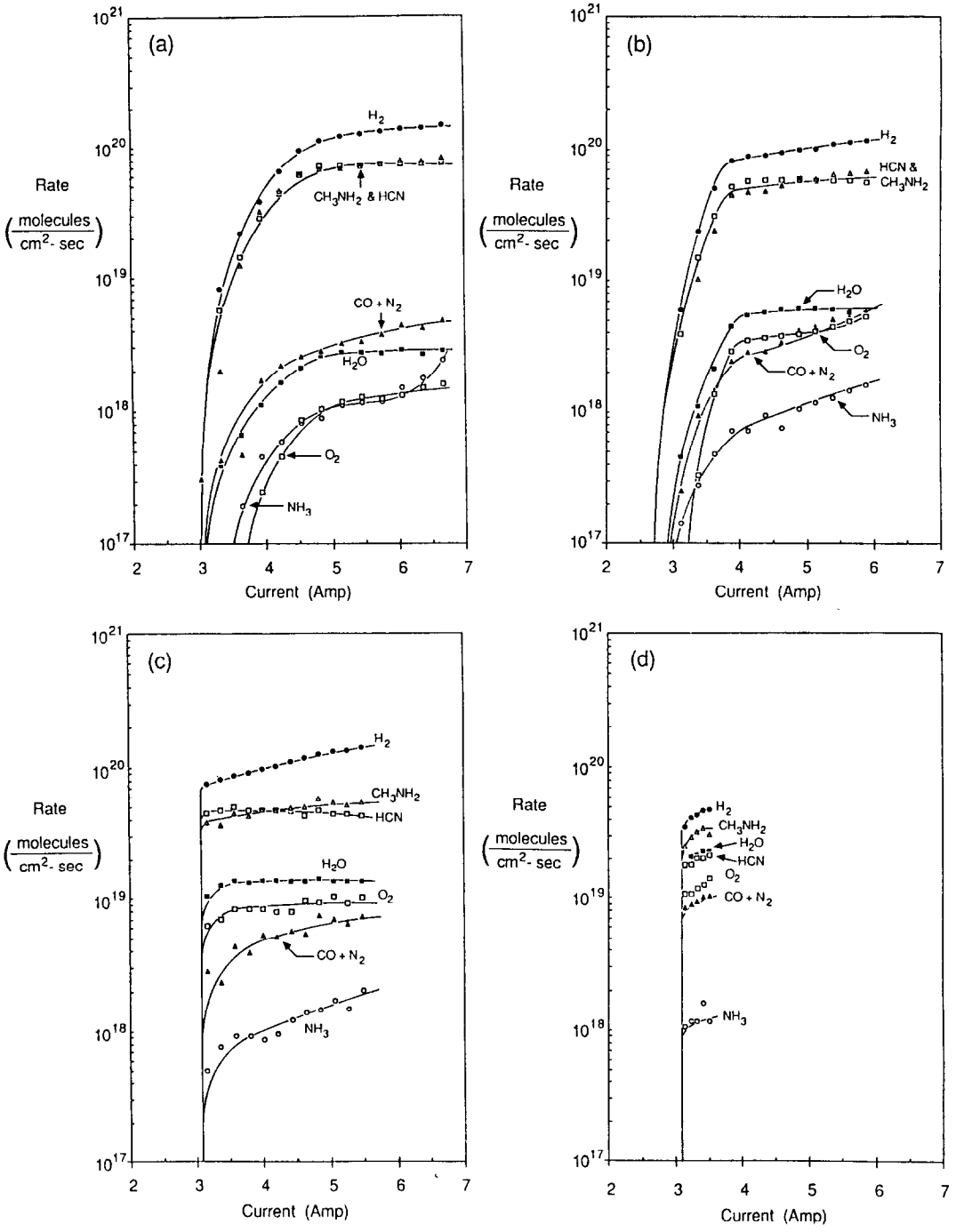

FIG. 1. Rate of consumption of CH_3NH_2 and O_2 and rates of formation of H_2, HCN, CO + N_2, H_2O, and NH_3 as functions of current through Pt wire in 2 Torr of CH_3NH_2 and (a) 0.25 Torr, (b) 1 Torr, (c) 2 Torr, and (d) 4 Torr of O_2.

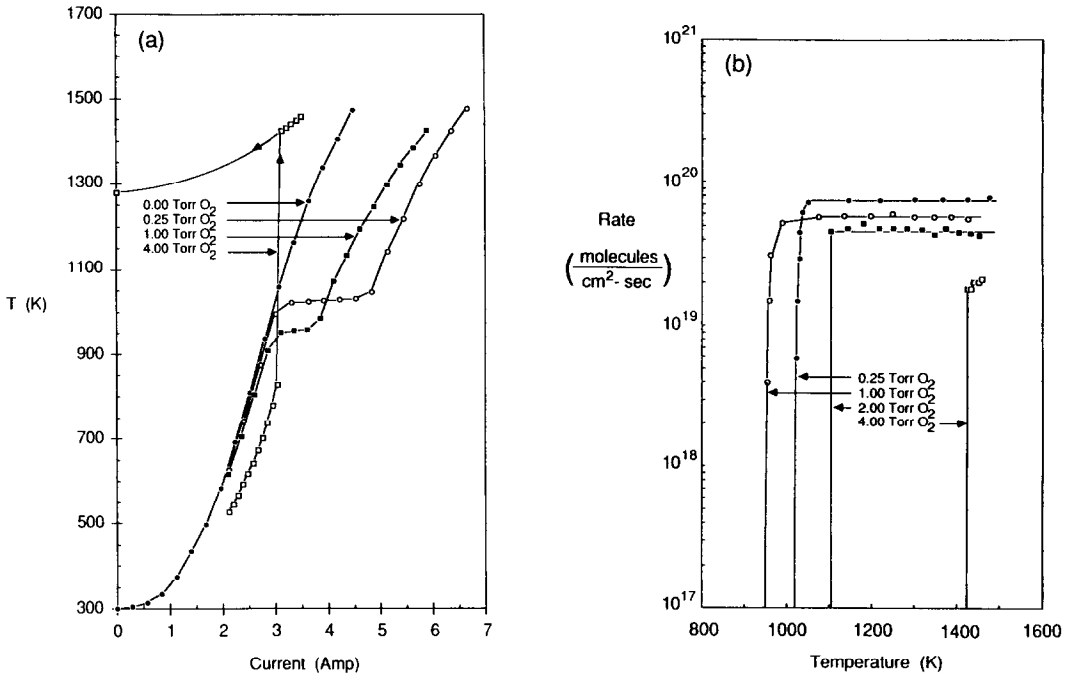

FIG. 2. (a) Temperature of the catalyst wire as a function of the current through the wire in 2 Torr of CH_3NH_2 and indicated oxygen partial pressures. (b) Rate of HCN formation as a function of wire temperature in 2 Torr of CH_3NH_2 and indicated oxygen partial pressures.

wire plotted as a function of applied current in 2 Torr of methylamine and indicated oxygen partial pressures. Figure 2b shows the rate of HCN formation under the same condition as a function of wire temperature. The temperatures shown in Fig. 2a for 0.25 and 1.0 Torr of oxygen were the average temperature of the wire (T_{avg}) calculated from the measured electrical resistance. The temperature at the middle of the wire (T_m) measured by thermocouple was close to T_{avg} shown in Fig. 2a up to where T_{avg} leveled off and increased slowly with increasing current (~1020 K at 0.25 Torr O_2 and ~950 K at 1.0 Torr O_2). It then went through a maximum and then a minimum and increased rapidly again after the reaction became flux-limited. This suggests that the temperature distribution along the wire was changed by the reaction: the endothermic reaction helped cool down the section at higher temperature (and higher reaction rate) and the temperature became more uniform along the wire. The reaction rates at 0.25 and 1.0 Torr of oxygen would become multivalued (S-shape) with respect to temperature if T_m rather than T_{avg} were used in Fig. 2b.

A macroscopic steady-state energy balance of the wire can be written as

$$I^2R = A\Sigma(r_i\Delta H_i) + UA(T - T_0) + A\varepsilon\sigma T^4 \quad (26)$$

with I the current on the wire, R the resistance of the wire, A the wire surface area, r_i the rate of ith reaction, U the heat transfer coefficient (to lead and to gas), ε the wire emissivity, and σ the Stefan–Boltzmann constant. With no oxygen at all, the wire became deactivated within a few minutes by a layer of carbon on the surface (shown by AES) and then no appreciable reaction would occur for a wire temperature up to 1450 K until activity was restored by heating in oxygen. At low temperatures, heat loss due to gas and lead conduction domi-

nates and the wire heats up roughly as I^2. At higher temperature, the radiation loss term (T^4) becomes important and the slope decreases. With only 0.25 or 1.0 Torr of oxygen, however, the temperature of the wire does not increase significantly after the reactions become significant due to the endothermic reaction until the reactions become flux-limited.

Due to the increased heat transfer coefficient U as the pressure increases, the wire has a lower temperature with 4 Torr of oxygen before the reactions are ignited. After the reactions are ignited, however, the wire temperature is more than 400° higher than at lower O_2 pressures, indicating that the overall reaction is now exothermic instead of endothermic. After the reactions are ignited at 4 Torr of O_2, the reactions maintain a steady-state temperature of 1280 K without any resistive heating. Figure 2b shows that in excess methylamine, reaction rate increases rapidly at some ignition temperatures, and little kinetic information can be gained from the rate versus temperature relationship in this regime.

3.2. *High-Temperature Kinetics*

At high temperature, rates become nearly independent of temperature, and effects of reaction heating and cooling do not interfere with rate measurements. In this section, we analyze the individual rates and orders in this regime in more detail. Figure 3a shows the reaction rate of all the reactants and detectable products at 1450 K, 4 Torr methylamine as functions of oxygen partial pressure. H_2 and HCN are the major products for the oxygen partial pressure range examined, constituting 98% of the product at low oxygen pressure and 75% at high oxygen pressure. Both H_2 and HCN follow CH_3NH_2 decomposition closely, again showing that reaction (1) is the major reaction. Rates of formation of CH_4 and NH_3 remain within 30% of each other and remain essentially independent of oxygen partial pressure. Reaction rates for O_2 consumption and H_2O formation both appear to be first order in the oxygen partial pressure with an H_2O rate about 30% higher than that of O_2. The rate of NO formation shows a second-order dependence on oxygen partial pressure while the rate of 28 amu (CO and N_2) formation appears to be zeroth order at low oxygen pressure and become first order at higher oxygen pressure.

Figure 3b shows the rates of methylamine and oxygen consumption as functions of oxygen pressure at methylamine pressures indicated. The rate of reaction of oxygen is clearly *independent of methylamine* and *first order in oxygen* partial pressure. A fit of the experimental data gives the rate of reaction of oxygen as

$$-r_{O_2} = 3.1 \times 10^{18} P_{O_2}. \qquad (27)$$

All rates are in units of molecules per square centimeter per second with partial pressures in Torr. Examination of Fig. 3b shows that the methylamine reaction rate is nearly *first order in methylamine* and *zeroth order in oxygen* at low oxygen pressure and becomes nearly second order in methylamine and minus first order in oxygen at high oxygen pressure. The following expression was found to fit the data:

$$-r_{CH_3NH_2} = \frac{2.7 \times 10^{19} P_{CH_3NH_2}}{1 + 0.647 P_{O_2}/P_{CH_3NH_2}}. \qquad (28)$$

Equation (28), a modified Langmuir–Hinshelwood rate expression, fits all data within 30% and satisfies the methylamine and oxygen pressure dependences observed. Figures 3c and 3d show the rates of formation of HCN and H_2 as functions of oxygen pressure, respectively. Since they follow closely the methylamine consumption, they are of course fit with same rate expression used for methylamine,

$$r_{HCN} = \tfrac{1}{2} r_{H_2} = -r_{CH_3NH_2}. \qquad (29)$$

Figure 3c also shows the reaction rate for 28 amu (CO and N_2) which appears to be close to first order in methylamine and independent of oxygen at low oxygen pressure and less than first order in methyl-

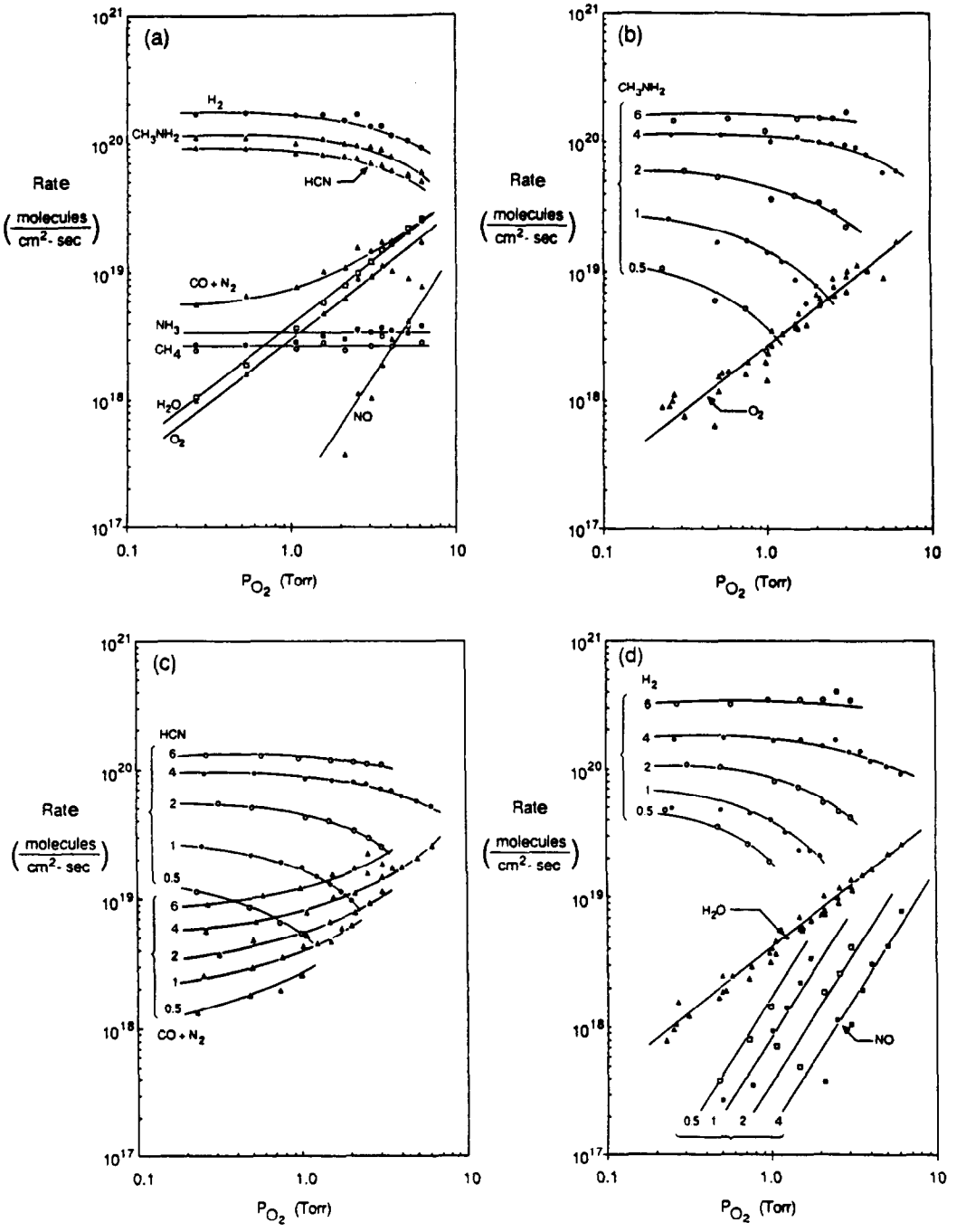

FIG. 3. (a) Rate of consumption of CH_3NH_2 and O_2 and rate of formation of H_2, HCN, CO + N_2, CH_4, H_2O, and NO as functions of oxygen partial pressure in 4 Torr of CH_3NH_2 at 1450 K. All pressures are in Torr. (b, c, d) Rate of consumption of CH_3NH_2 and O_2, and formation of HCN and CO + N_2, and H_2, and H_2, H_2O, and NO, respectively, as functions of oxygen partial pressure at 1450 K at indicated CH_3NH_2 pressures.

amine and first order in oxygen at high oxygen pressure. The following expression was found to fit the experimental data within 25%:

$$r_{CO+N_2} = 1.60 \times 10^{18} P_{CH_3NH_2} + 2.53 \times 10^{18} P_{O_2}. \quad (30)$$

The first term on the right-hand side of Eq. (30) represents the rate of formation of nitrogen and is proportional to the amine pressure while the second term represents that of CO and is proportional to the oxygen pressure. The rate of water and nitric oxide formation shown in Fig. 3d can be fit as

$$r_{H_2O} = 4.3 \times 10^{18} P_{O_2} \quad (31)$$

$$r_{NO} = 6 \times 10^{17} P_{O_2}^2 / P_{CH_3NH_2}. \quad (32)$$

Ammonia and methane together constitute less than 3% of the product and are both first order in methylamine and independent of oxygen. Their reaction rates could be fit within 40% with the rate expressions

$$r_{CH_4} = 6.85 \times 10^{17} P_{CH_3NH_2} \quad (33)$$

$$r_{NH_3} = 7.42 \times 10^{17} P_{CH_3NH_2}. \quad (34)$$

The amount of CO_2 formed in the reaction appears to increase with both amine and oxygen partial pressures but is always lower than that of methane and was not quantified. With Eqs. (27) through (34), overall mass balances for H, C, N, and O atoms show that all species were balanced within 30%. Figure 4a shows that excellent agreement between experimental data and Eqs. (27) to (34) (solid curves) was obtained for 2 Torr of methylamine.

Figure 4b shows the experimental selectivity for HCN formation as a function of $P_{O_2}/P_{CH_3NH_2}$ ratio together with the theoretical value calculated from Eqs. (29) and (30). Both the experimental data and the calculated curve indicate a dramatic decrease in

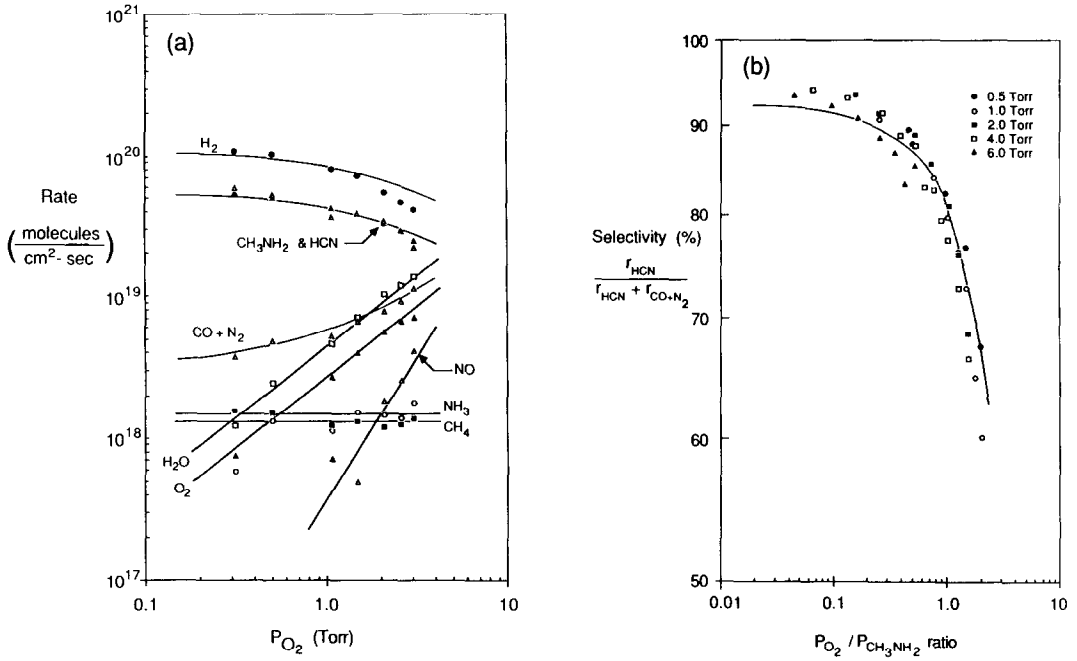

FIG. 4. Comparison between the experimental data and rates calculated from rate expressions described in text (solid curves) in 2 Torr of CH_2NH_2, 1450 K. (b) Experimental selectivity for HCN formation and that calculated from rate expressions (solid curve) at 1450 K as functions of O_2/CH_3NH_2 ratio.

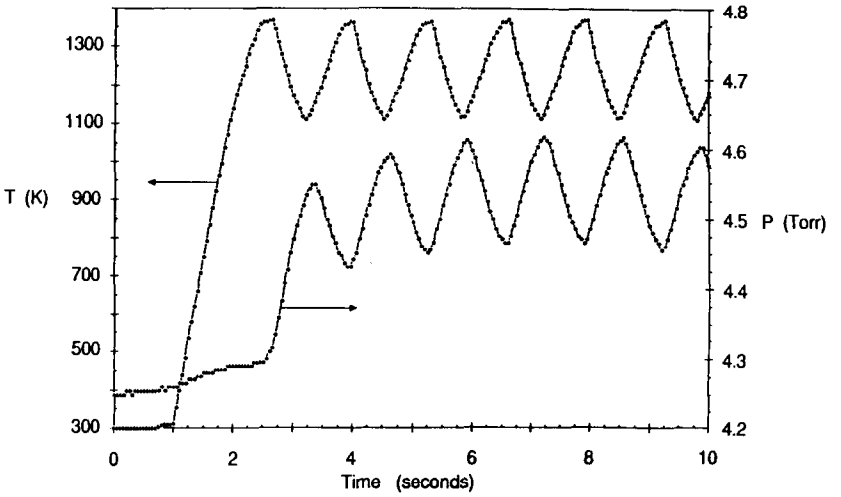

FIG. 5. Temperature and pressure oscillations in 4 Torr of CH_3NH_2 and 0.25 Torr of O_2 with a residence time of 0.92 s. At $t = 1$ s, a dc current was applied to the wire initially at room temperature.

selectivity of HCN for $P_{O_2}/P_{CH_3NH_2}$ ratio above 0.5. However, all selectivities observed and calculated are above 60% for HCN even under highly oxidative conditions. The data appear to be higher at low $P_{O_2}/P_{CH_3NH_2}$ ratio and lower at high $P_{O_2}/P_{CH_3NH_2}$ ratio than the calculated curve. Experimental selectivities also decrease with increasing amine pressure, while the calculated curve is a unique function of the $P_{O_2}/P_{CH_3NH_2}$ ratio.

3.3 Temperature and Pressure Oscillations

Simple periodic and complex oscillations in catalyst temperature and reaction species concentrations have been observed in several reaction systems under steady inlet flow conditions (*31–37*). In a recent review, Razon and Schmitz (*31*) listed 14 reaction systems known to give oscillatory responses in the oxidation of CO, H_2, NH_3, C_2H_4, C_3H_6, CH_3OH, C_6H_{12}, and CH_3CH CH_2O, in N_2O decomposition, and in CO + H_2, NO + CO, NO + NH_3, and C_2H_2 + H_2 reaction. Oxidations of H_2 and CO (*33–36*) are probably the simplest systems because they presumably involve a small number of intermediates, and the reaction conditions have been almost isothermal. While these reactions have been subjected to extensive studies, no generally accepted explanation for them has appeared.

Flytzani-Stephanopoulos *et al.* (*15*) reported simple and complex oscillations in NH_3 oxidation at a reactant pressure of 1 atm with period from <1 s to several minutes for 20–40% NH_3 in air (excess NH_3) over Pt wires and foils. They found the homogeneous reaction to be responsible for the oscillations at high gas temperature and suggested that an interplay between the endothermic decomposition and the exothermic oxidation reactions may cause the oscillation in excess ammonia. However, they were unable to determine whether coupling between chemical and physical processes was necessary for the appearance of oscillations.

In this study, oscillatory temperature and pressure are also observed in excess methylamine and appear to be caused by the endothermicity of the decomposition reaction. Homogeneous reactions do not occur in our reaction system because of lower pressure and consequent wall cooling of gases and quenching of any intermediates which could cause homogeneous propagation. In Fig. 5, the wire initially at room temperature was exposed to 4 Torr of

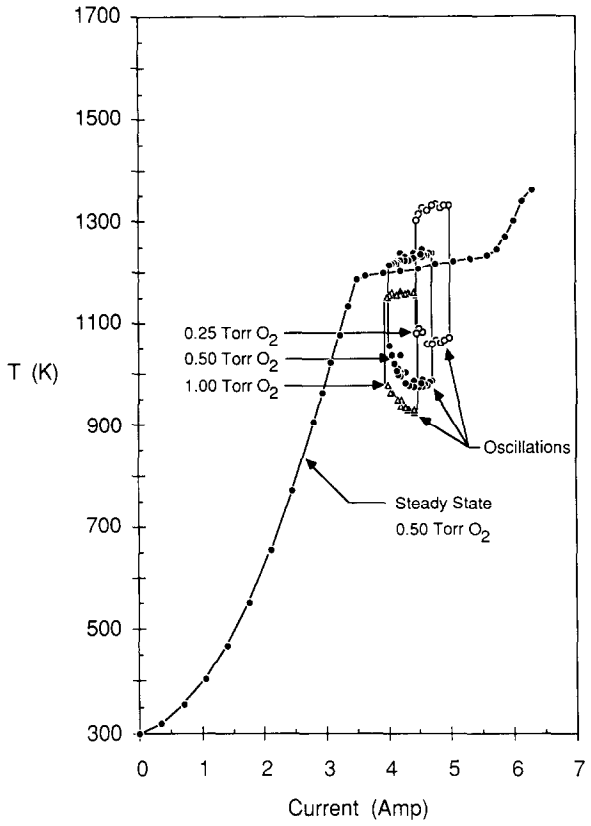

FIG. 6. The regime where oscillations were observed and the maximum and minimum of wire temperature during oscillation in 4 Torr of CH_3NH_2 at O_2 partial pressures indicated. The solid curve shows the steady-state temperature of the wire upon gradually increasing the current.

methylamine and 0.25 Torr of oxygen with a residence time less than one second. A dc current was then applied to heat up the wire and the oscillation began with 2.5 s. The temperature of the wire started to oscillate with a period of 1.32 s and an amplitude of 270 K immediately after the wire reached the maximum temperature of the oscillation. The pressure in the reactor did not respond to heating until the wire temperature reached its maximum and started to oscillate. The pressure then oscillated with an amplitude of 0.164 Torr and the same period of the wire but with more than a 180° phase lag. Oscillations similar to this were reproduced on several different Pt wires and were observed to be sustained for more than 1 h with no detectable change in period, amplitude, or peak shape. Oscillations were observed only in a narrow regime of composition and temperature with periods and amplitudes dependent on methylamine and oxygen pressures and residence time. For 4 Torr of methylamine, oscillations were observed between 0.25 and 1.5 Torr of oxygen.

The wire could be made to exhibit either a stable state or oscillations at a particular temperature, depending on previous temperature–time conditions. As shown in Fig. 6, upon slowly increasing the current through the wire in 4 Torr of methylamine and 0.5 Torr of oxygen (solid curve), the wire temperature rose smoothly, rose more slowly after the reaction was ignited, and then rose rapidly again after the reactions became flux-limited, with no oscillatory behavior observed. However, when a con-

stant current between 4.1 and 4.7 A was suddenly applied to a wire initially at room temperature, oscillations such as those shown in Fig. 5 began. The same oscillation behavior could also be obtained by first heating the wire to ~1500 K and then reducing the current to the previous setting. Figure 6 also shows the oscillatory regimes (but not steady-state regimes) for 4 Torr of methylamine with 0.25 and 1.0 Torr of oxygen with points indicating the observed maximum and minimum wire temperature.

4. DISCUSSION

4.1. Reactions and Rates

From Figs. 3 and 4, it is clear that the major reaction in a mixture of methylamine and oxygen is *methylamine decomposition to HCN*. The rates of formation of HCN and H_2 follow closely the rate of consumption of methylamine under all experimental conditions, suggesting that the addition of oxygen does not significantly change the chemistry of reactions of the C–N bond in methylamine. The rate of HCN formation *decreases* with increasing oxygen partial pressure simply due to the *competitive adsorption* of methylamine and oxygen. At lower oxygen partial pressures, the oxygen acts primarily as a scavenger to prevent formation of carbon on the catalyst. We suspect that this is due to decomposition of traces of di- and trimethylamine, which leave excess carbon after reaction. Even a small amount of O_2 (~50/1 excess CH_3NH_2) appears to be able to oxidize this carbon which otherwise inhibits CH_3NH_2 decomposition. At higher oxygen partial pressures, oxygen oxidizes H_2, NH_3, and a small fraction of the CH_3NH_2 to give H_2O, NO, and CO.

Since many of the reactions listed in Table 1 have been studied (*20–30*) and rate expressions on Pt foils or wires have been developed, we can use these rate expressions to evaluate the possible contribution from these reactions. In Table 2, the first row shows the rate of formation of different species and the rate of consumption of oxygen observed in a mixture of 1 Torr methylamine and 1 Torr oxygen over Pt wire at 1450 K. The partial pressures of the products and oxygen were calculated from the observed reaction rate and then used to calculate the rates of the reactions listed. Of the 15 reactions listed in Table 2, only two reactions, the ammonia oxidation to NO and hydrogen oxidation, have reaction rates sufficiently large to approach the experimental rate of formation. All the other reactions have predicted reaction rates more than one order of magnitude lower than the experimental data and are therefore insignificant in this system.

The rate of NO formation calculated from the ammonia oxidation reactions is about 0.4 of the experimental rate of NO formation and should be first order in ammonia and $\frac{1}{2}$ order in oxygen partial pressure under these experimental conditions (*22*). Since the ammonia partial pressure increase is directly proportional to the methylamine pressure decrease by Eq. (*34*), the NO formation then becomes first order in methylamine and $\frac{1}{2}$ order in oxygen partial pressure. Although this is quite different from the observed dependences (second order in oxygen and minus first order in methylamine), the discrepancy may be due to different experimental conditions (10–90% NH_3 in O_2, total pressure <1 Torr used by Pignet and Schmidt (*22*), compared to a ~50/1 excess O_2, total pressure >1 Torr in this study), so that ammonia oxidation may still be the major source of NO formation.

The rates of water formation and oxygen consumption calculated from the hydrogen oxidation reaction are both within a factor of 1.5 of the experimental data. Although the reaction should be first order in oxygen and hydrogen partial pressures (*30*) for mixtures near stoichiometry, it may become limited by adsorption of oxygen in our experiments due to the low sticking coefficient of oxygen at high temperature and the large amount of atomic hydrogen produced on the surface by methylamine decomposi-

TABLE 2

Comparison of Rates[a] with Literature Values[b]

Species	H_2	CH_4	NH_3	H_2O	HCN	$CO + N_2$	NO	O_2	CO_2	Reference
Total rate	5×10^{19}	1×10^{18}	9×10^{17}	3×10^{18}	2×10^{19}	4×10^{18}	1×10^{18}	-3×10^{18}	4×10^{17}	This work[c]
$4NH_3 + 5O_2 \rightarrow 4NO + 6H_2O$			-4×10^{17}	6×10^{17}			4×10^{17}	5×10^{17}		(*21, 22*)
$4NH_3 + 3O_2 \rightarrow 2N_2 + 6H_2O$			-1×10^{16}	2×10^{16}		5×10^{15}		-7×10^{15}		(*21, 22*)
$2CH_4 + 3O_2 \rightarrow 2CO + 4H_2O$		-3×10^{16}		6×10^{16}		3×10^{16}		-5×10^{16}		(*20*)
$CH_4 + 2O_2 \rightarrow CO_2 + 2H_2O$		-2×10^{16}		4×10^{16}				-4×10^{16}	2×10^{16}	(*20*)
$2H_2 + O_2 \rightarrow 2H_2O$	-4×10^{18}			4×10^{18}				2×10^{18}		(*30*)
$2CO + O_2 \rightarrow 2CO_2$						-7×10^{10}		-4×10^{10}	7×10^{10}	(*28, 30*)
$2NO + 2H_2 \rightarrow N_2 + 2H_2O$	-1×10^{16}			1×10^{16}		5×10^{15}	-1×10^{16}			(*27*)
$CO + H_2O \rightarrow CO_2 + H_2$	4×10^{15}			-4×10^{15}		-4×10^{15}			4×10^{15}	(*30*)
$2NH_3 \rightarrow N_2 + 3H_2$	5×10^{16}		-3×10^{16}			2×10^{16}				(*20, 25*)
$2NO \rightarrow N_2 + O_2$						2×10^{12}	-3×10^{12}	2×10^{12}		(*26, 27*)
$6NO + 4NH_3 \rightarrow 5N_2 + 6H_2O$			-3×10^{15}	5×10^{15}		4×10^{15}	-5×10^{15}			(*29*)
$CH_4 + NH_3 \rightarrow HCN + 3H_2$	1×10^{16}	-3×10^{15}	-3×10^{15}		3×10^{15}					(*20, 23*)
$2CH_4 + 6NO \rightarrow 3N_2 + 2CO + 2H_2O$		-2×10^{15}		2×10^{15}		5×10^{15}	-6×10^{15}			(*20*)
$2CH_4 + 2NO \rightarrow H_2 + 2HCN + 2H_2O$	5×10^{14}	-1×10^{15}		1×10^{15}	1×10^{15}		-1×10^{15}			(*20*)
$2NO + 2CO \rightarrow N_2 + 2CO_2$						-2×10^{16}	-4×10^{16}		2×10^{16}	(*24, 28*)

[a] All rates in molecules per square centimeter per second.
[b] The predicted reaction rates were calculated by the rate expressions in the references with partial pressure of species measured in 1 Torr methylamine and 1 Torr oxygen.
[c] Measured in 1 Torr CH_3NH_2 and 1 Torr O_2 at 1450 K.

tion. The reaction rate then would become first order in oxygen and independent of hydrogen or methylamine partial pressures. In a recent paper, Zhdanov (*38*) showed that the rate of water formation becomes independent of hydrogen partial pressure in excess hydrogen on Pt(111) for $T > 700$ K. Most of the oxygen reacted formed H_2O (~70%) and the rest formed NO, CO, and CO_2.

4.2. *Mechanism of Oscillations*

Although this reaction system involves at least two known oscillatory reactions (NH_3 oxidation and $H_2 + O_2$), oscillations at these temperatures and pressures appear to be largely due to the dynamics of the wire temperature. The ammonia oxidation was reported to be oscillatory, but only at atmospheric pressure (*15, 31, 37*), not at a total pressure of ~1 Torr (*21, 22*). The oscillations observed in hydrogen oxidation on Pt wires and foils are usually at low temperature and have much longer periods of 1 to 120 min.

The temperature and pressure oscillations observed in this study appear to be explainable qualitatively by considering the dynamics of the catalyst wire. Upon a gradual increase in the current through the wire, the wire temperature increased slowly from the ignition temperature to the temperature where reaction became flux-limited. The system could then reach stable steady state without oscillations. When a wire initially at room temperature was suddenly brought to a temperature above the ignition temperature, the reaction rate increased rapidly (Fig. 2) and the wire then cooled rapidly by the endothermic reaction. The wire then went through a maximum temperature (determined by the balance between resistive heating and the endothermic reaction of Eq. (26)) and cooled to below the ignition temperature where the reaction was quenched. It then returned to above the ignition temperature by resistive heating and another cycle of oscillation began.

Examination of the temperature response in Fig. 5 reveals that the wire heats up during the oscillation at the same rate as it does before the oscillation. This indicates that the wire heats up primarily due to resistive heating during the oscillation, suggesting that the temperature and pressure oscillation are due to the interaction between the endothermic reaction and the resistive heating. The pressure variations shown in Fig. 5 indicate that the above explanation is plausible. The pressure rose shortly after the wire reached the ignition temperature and kept increasing until the wire cooled to the minimum temperature. The pressure then started to fall (since the reaction stopped) until the wire exceeded the ignition temperature again due to resistive heating. After the reaction was ignited, the pressure did not fall back to the pressure before the reaction because of the long pumping time constant of the reactor even though the reaction was quenched some time during the period. Since the wire did not heat up and cool down uniformly during the oscillation and the reaction changed the temperature distribution along the wire (3.1), any quantitative characterization of the oscillation would have to include the temperature distribution along the wire.

4.3. CH_3NH_2 *versus* NH_3

The oxidation of ammonia to NO is important in the chemical industry for the production of nitric acid. It is catalyzed by platinum and its alloys and is one of the most exothermic chemical reactions (*18*). Over the past 60 years, this system has been the object of a great number of studies (*21*). Recently, its kinetics has been studied on Pt wires in the range 0.1–1 Torr (*21, 22*) and on Pt single-crystal surfaces in the range 10^{-10}–10^{-8} Torr (*16–18*).

Pignet and Schmidt (*21, 22*) studied the reaction between 200 and 1400°C over Pt, Rh, and Pd polycrystalline wires. They modeled the reactions as a simple series-parallel mechanism with three individual surface reaction steps which can be modeled by classical Langmuir–Hinshelwood

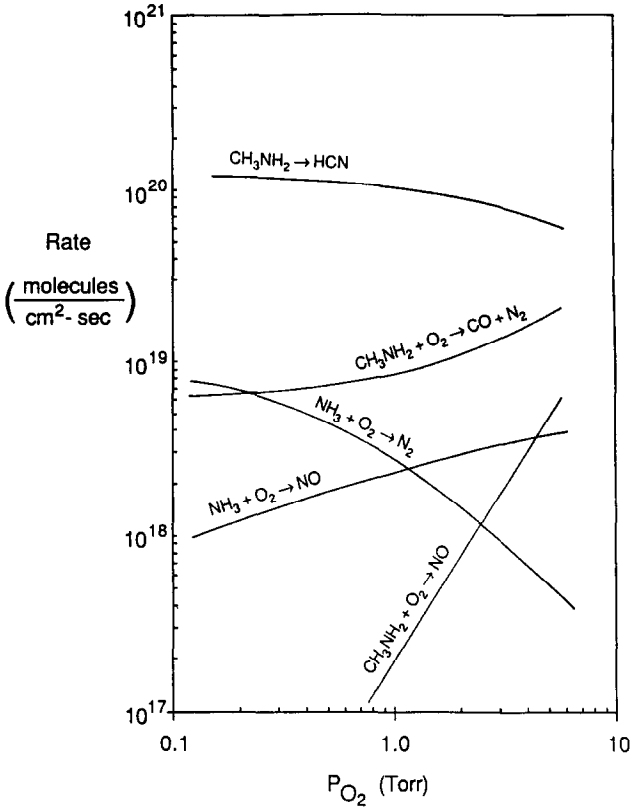

FIG. 7. Rate of N_2 and NO formation in ammonia oxidation calculated from Ref. (*22*) in 4 Torr of NH_3 and rate of HCN, N_2, and NO formation in 4 Torr of CH_3NH_2 at 1450 K as functions of oxygen partial pressure. Since the rate of formation of N_2 from NH_3 depends on NO partial pressure, the maximum NH_3 to NO conversion was assumed to be 10%.

kinetic forms. Kinetics measured at low pressure (0.1–1 Torr) were used to estimate selectivities of NO and N_2 production under conditions of industrial nitric acid production. The predicted selectivity, optimum temperature, and composition matched closely those observed in the high-pressure (1–8 atm) process.

Figure 7 shows the rate of formation of NO and N_2 as functions of oxygen pressure at 4 Torr of ammonia from ammonia oxidation over Pt wire at 1450 K calculated from the rate expressions given by Pignet and Schmidt (*22*). Since the rate of formation of N_2 depends strongly on NO partial pressure, the maximum NO conversion is assumed to be 10%. The rate of NO formation is almost independent of NH_3 and is about $\frac{1}{2}$ order in oxygen partial pressure. The rate of N_2 formation is about first order in ammonia and minus first order in oxygen partial pressure. The N_2 formation rate at the lowest oxygen partial pressure is close to that calculated from the decomposition of pure NH_3 (*25*).

The most striking difference between the rates of methylamine oxidation and ammonia oxidation is that *methylamine decomposes more than 10 times faster than ammonia* under similar conditions. This is also seen in that methylamine decomposition is flux-limited (Fig. 2) but the ammonia decomposition (*25*) and oxidation (*22*) are not. The rate of NH_3 oxidation exhibits a temperature maximum and a large decrease at high temperature. The presence of oxygen

evidently inhibits the decomposition of ammonia much more than that of methylamine in that twofold excess of O_2 reduces the $NH_3 \rightarrow N_2$ reaction rate by a factor of 12 but reduces the $CH_3NH_2 \rightarrow HCN$ reaction rate only by a factor of ~2.

In a recent paper (*9*) we studied the methylamine decomposition on Pt(111) and associated the difference between CH_3NH_2 and NH_3 with the stability of the C–N multiple bonds from CH_3NH_2. In methylamine decomposition in the presence of oxygen, CH_3NH_2 molecule simply dehydrogenates to HCN and desorbs since the oxygen does not break the C–N bond in CH_3NH_2, while for ammonia oxidation, N_2 is formed either from complete dehydrogenation of NH_3 followed by recombination of surface N atoms (*25*) or from reaction between NH_3 and NO which is formed by the $NH_3 + O_2$ reaction (*22*).

SUMMARY

Methylamine decomposition to HCN and H_2 was found to be the major reaction in $CH_3NH_2 + O_2$ mixtures, while oxidations of hydrogen and ammonia are primarily responsible for formation of H_2O and NO, respectively. At low oxygen partial pressures, the oxygen acts primarily as a scavenger to prevent formation of a carbon layer which would otherwise passivate the catalyst. At higher oxygen partial pressures, oxygen oxidizes H_2, NH_3, and a small fraction of the CH_3NH_2 to form H_2O, NO, and CO. In excess methylamine, the overall reaction is endothermic and the reaction rates increase rapidly at ~950 K with most reactions becoming flux-limited at ~1100 K. In excess oxygen, the overall reaction becomes exothermic and autothermal above 1000 K.

The rate and order of the formation or consumption of individual species have been examined in detail at 1450 K where most reactions are flux-limited. Rates of consumption of CH_3NH_2 and O_2 and rates of formation of HCN, H_2, CO + N_2, H_2O, NH_3, CH_4, and NO were fit with modified Langmuir–Hinshelwood, first-order rate expressions with good agreement (Fig. 4).

The temperature of the wire and the pressure in the reactor were found to oscillate in excess CH_3NH_2 under certain conditions. This appears to be attributable to the interaction between the resistive heating and the endothermic decomposition reaction. The rate of CH_3NH_2 decomposition was found to be more than 10 times faster than ammonia oxidation. The difference may be associated with the stability of the C–N bond in CH_3NH_2 on Pt surfaces.

ACKNOWLEDGMENT

The authors thank Professor Raul A. Caretta for helpful discussions concerning the manuscript.

REFERENCES

1. Sabatier, P., and Gaudion, G., *C.R. Acad. Sci. Paris* **165,** 309 (1917).
2. Emmett, P. H., and Harkness, R. W., *J. Amer. Chem. Soc.* **54,** 538 (1932).
3. Kemball, C., and Moss, R. L., *Proc. R. Soc. London Ser. A* **238,** 107 (1956).
4. Kemball, C., and Moss, R. L., *Proc. R. Soc. London Ser. A* **244,** 398 (1958).
5. Kemball, C., and Moss, R. L., *Trans. Faraday Soc.* **56,** 154 (1960).
6. Anderson, J. R., and Clark, N. J., *J. Catal.* **5,** 250 (1966).
7. Orita, H., Naito, S., Onishi, T., and Tamaru, K., *Bull. Chem. Soc. Japan* **56,** 3390 (1983).
8. Meitzner, G., Mykytka, W. J., and Sinfelt, J. H., *J. Catal.* **98,** 513 (1986).
9. Hwang, S. Y., Seebauer, E. G., and Schmidt, L. D., *Surf. Sci.* **188,** 219 (1987).
10. Bridge, M. E., and Somers, J., submitted for publication.
11. Chorkendorff, I., Russell, N. J., Jr., and Yates, J. T., Jr., *J. Chem. Phys.* **86,** 4692 (1987).
12. Pearlstine, K. A., and Friend, C. M., *J. Amer. Chem. Soc.* **108,** 5842 (1986).
13. Walker, B. W., and Stair, P. C., *Surf. Sci.* **103,** 315 (1981).
14. Baca, A. G., Schulz, M. A., and Shirley, D. A., *J. Chem. Phys.* **83,** 6001 (1985).
15. Flytzani-Stephanopoulos, M., Schmidt, L. D., and Caretta, R., *J. Catal.* **64,** 346 (1980).
16. Gland, J. L., and Korchak, V. N., *J. Catal.* **53,** 9 (1978).
17. Gland, J. L., Woodard, G. C., and Korchak, V. N., *J. Catal.* **61,** 543 (1980).

18. Asscher, M., Guthrie, W. L., Lin, T.-H., and Somorjai, G. A., *J. Phys. Chem.* **88,** 3233 (1984).

19. Selwyn, G. S., and Lin, M. C., *Langmuir* **1,** 212 (1985).

20. Hasenberg, D., and Schmidt, L. D., *J. Catal.* **104,** 441 (1987).

21. Pignet, T. P., and Schmidt, L. D., *Chem. Eng. Sci.* **29,** 1123 (1974).

22. Pignet, T. P., and Schmidt, L. D., *J. Catal.* **40,** 212 (1975).

23. Hasenberg, D., and Schmidt, L. D., *J. Catal.* **97,** 156 (1986).

24. Klein, R. L., Schwartz, S. B., and Schmidt, L. D., *J. Phys. Chem.* **89,** 4908 (1985).

25. Löffler, D. G., and Schmidt, L. D., *J. Catal.* **41,** 440 (1976).

26. Mummy, M. J., and Schmidt, L. D., *Surf. Sci.* **109,** 29 (1981).

27. Papapolymerou, G. A., and Schmidt, L. D., *Langmuir* **1,** 488 (1985).

28. Schwartz, S. B., Schmidt, L. D., and Fisher, G. B., *J. Phys. Chem.* **90,** 6194 (1986).

29. Takoudis, C. G., and Schmidt, L. D., *J. Phys. Chem.* **87,** 958, 965 (1983).

30. Blieszner, J., Ph.D. thesis, University of Minnesota, 1979.

31. Razon, L. F., and Schmitz, R. A., *Catal. Rev. Sci. Eng.* **28,** 89 (1986).

32. Sheintuch, M., and Schmitz, R. A., *Catal. Rev. Sci. Eng.* **15,** 107 (1977).

33. Lindstrom, T. H., and Tsotsis, T. T., *Surf. Sci.* **171,** 349 (1986).

34. Elswirth, M., and Ertl, G., *Surf. Sci.* **177,** 90 (1986).

35. Zuniga, J. E., and Luss, D., *J. Catal.* **53,** 312 (1978).

36. Saidi, G., and Tsotsis, T. T., *Surf. Sci.* **161,** L591 (1985).

37. Edwards, W. M., Zuniga-Chaves, J. E., Worley, F. L., Jr., and Luss, D., *AIChE J.* **20,** 571 (1974).

38. Zhdanov, V. P., *Surf. Sci.* **169,** 1 (1986).